A Multi Objective Genetic Algorithm (MOGA) for Optimizing Thermal and Electrical Distribution in Tumor Ablation by Irreversible Electroporation

Nickfarjam A.[1], Firoozabadi S. M. P.[1]*, Kalaghchi B.[3]

[1]Tarbiat Modares University, Medical Physics Department, Tehran, Iran
[2]Cancer Research Center, Tehran University of Medical Sciences, Tehran, Iran

ABSTRACT

Background: Irreversible electroporation (IRE) is a novel tumor ablation technique. IRE is associated with high electrical fields and is often reported in conjunction with thermal damage caused by Joule heating. For good response to surgery it is crucial to produce minimum thermal damage in both tumoral and healthy tissues named Non-Thermal Irreversible Electroporation(NTIRE). Non-thermal irreversible electroporation attempts have concentrated on tumor ablation with strong electric field with producing minimum thermal damage.

Objective: To establish a Multi Objective Genetic Algorithm (MOGA) for IRE treatment planning.

Methods: Numerical modeling and genetic programming were coupled to optimize thermal and electrical distribution in tissue. A 3D MRI based model was established and treatment parameters such as electrode thickness, electrode insertion, distance between electrode and applied voltage were optimized.

Results: Prefect tumor ablation with IRE surgery with relatively little electrical and thermal damage on healthy tissue can be achieved by using genetic algorithm optimization. Such optimization can trade off between perfect tumor coverage and damage to healthy tissue. Concerning the thermal aspect of IRE surgery.

Conclusion: The established multi-objective genetic algorithm based treatment planning system, can optimize both geometric and electric parameters in IRE surgery. Such optimization result in prefect tumor ablation as well as minimum thermal damage to both normal and tumoral tissue.

Keywords

Irreversible electroporation, Tumor ablation, Genetic algorithm, Finite element method, Numerical modeling

Introduction

Tissue ablation is the resection of unhealthy tissue with the aim to cure a disease. This method is one of the modalities used in cancer treatment. Ablation of tumor (or undesirable tissue) often is performed via thermal method. Laser, ultrasound, radiofrequency electric current and microwaves are different physical principles that can be employed for heating tissue [1]. In addition to the methods listed, recently a new method called irreversible electroporation (IRE) has been introduced in order to destroy unhealthy tissues. In general, electro-

*Corresponding author: Firoozabadi S. M. P. Tarbiat Modares University, Medical Physics Department, Tehran, Iran
E-mail: pourmir@modares.ac.ir

poration is a method to increase permeability of cells using electric fields [2, 3]. Respect to strength of electric field, the electroporation of cells can be reversible or irreversible. Unlike reversible electroporation (RE), in IRE strong electric field is used and consequently lead to permanent permeabilization of tissue's cells. RE mainly used in electrochemotherapy and electrogenetherapy. Several teams proved that IRE can ablate undesired tissue [1-3]. But the main point that must be considered is minimal damage to normal tissue. Since strong electric fields are used in IRE, the ablated area can be extended to normal tissue. Ablation of tissue via IRE procedure can be performed in electrical or thermal manner. For instance if electric field is greater than 900 V/cm, the target tissue can irreversibly electroporated (electrical manner). In addition; this electric field can produce heat (joule heating) and this heat regardless of electric distribution, can ablate target tissue similar to other thermal ablation tumor methods. But IRE surgery on animal tissue shows that non-thermal IRE (NTIRE) has many beneficial effects such as extremely rapid regeneration of ablated tissue with healthy tissue without scar formation, inducing a good immune response [4], allowing treatment in the heart [5] and blood vessels [6] without the danger of coagulation and subsequent emboli.

Several studies have shown that numerical modeling can be used to estimate the electric and thermal distribution in tissue[7-10]. Moreover, the outcome of treatment prediction before its implementation in order to select the best treatment parameters is commonly used in radiotherapy named treatment planning. This study has been done to design a treatment planning system for IRE tumor ablation.

In this study we coupled numerical modeling and genetic programming to optimize electrode configuration to optimum thermal and electric distribution in healthy and unhealthy tissue. A 3D MRI based model used for numerical modeling ; we used multi-objective optimization in genetic programming to consider both electric and thermal effect on tissue. Such optimization leads to minimally invasive tissue ablation as well as minimum joule heating.

Materials and Methods

Numerical modeling

In order to numerically evaluate of the electric distribution in the tissues, Laplace equation was used [7, 11]:

$$-\nabla.(\sigma\nabla\varphi)=0 \qquad (1)$$

where σ and φ stand for the electric conductivity of the tissue and electric potential, respectively. It should be noted that by solving above equation, the electric field distributions was obtained in the model. Boundary between reversible and irreversible electroporation for subcutaneous tumor is 900 V/cm[12], which is used as the criteria for calculating reversible and irreversible volume. This value is taken from a previously published study[13, 14].

A modified Pennes (bioheat) equation was used to determine temperature distribution. In order to consider the heat generated from the IRE procedure, Joule heating $(\sigma|\nabla\varphi|^2))$ is added to the original Pennes equation[15]:

$$\nabla.(k\nabla T)+\omega_b c_b(T_a-T)+q'''+\sigma|\nabla\varphi|^2=\rho c_p\frac{\partial T}{\partial t} \qquad (2)$$

where k stands for the thermal conductivity of the tissue, T is the temperature, ω_b is the blood perfusion, c_b is the heat capacity of the blood, T_a is the arterial temperature, q'''is the metabolic heat generation, ρ is the tissue density, and c_p is the heat capacity of the tissue.

The constant parameters in equations 1 and 2 that used in the model are summarized in Table 1.

In order to calculate thermal damage Ω, Arrhenius equation was used [7, 16]:

$$\Omega=\int\xi e^{-\frac{E_a}{RT}}dt \qquad (3)$$

Table 1: Electrical and thermal constant used in the model.

Tissue/ Electrode Quantity	Healthy tissue	Tumor	Electrode (Aluminum)
Electric conductivity-(S/m)	0.41[17]	0.4[12]	3.774×10^{7}
Thermal conductivity-k(W/m.K)	0.5[17]	0.75[18]	250
Specific heat-c(J/kg.K)	3800[19]	3700[20]	910
Blood perfusion rate-(1/s)	6.557×10^{-4}[21]	2×10^{-3}[18]	------
Metabolic heat source-(W/m^3)	800[19]	42000[18]	------
Density-(kg/m^3)	1040[17]	1050[20]	2700

in which ξ is the frequency factor in 1/s, E_a is the activation energy in Joule/mole, R is the universal gas constant (Joule/mole.Kelvin), and T is the absolute temperature in Kelvin.

The finite element method (FEM) was used to solve partial differential equations (eq. 1,2) . All finite element analyses were performed using the commercial finite element package Femlab v3.5a (Comsol AS, Stockholm, Sweden). The Convergence test was performed to ensure adequate mesh density and validity of simulation. To this end, the number of elements in the FE model was increased and electric potential was calculated for the model. When simulated electric potential converged, that is, it changed by less than 1%, the convergence process defined the number of elements in the model.

Boundary and initial conditions

To solve eq. (1), it is assumed that electrical boundary condition of electrode is

$$\varphi = V_0 \qquad (4)$$

The electrical boundary condition at the outer surface of tissue is electrically insulative, it means:

$$\frac{\partial \varphi}{\partial n} = 0. \qquad (5)$$

To solve eq. (2), the outer surface domains are considered as adiabatic to predict the maximum temperature rise in tissue [7,11]:

$$\frac{\partial T}{\partial n} = 0 \qquad (6)$$

Furthermore, it is assumed that the initial temperature value of tissue is physiological temperature of 37° C.

The calculations were made using an electroporation pulse of 0.1 ms. Because typically reversible and irreversible electroporation is done with eight to ten 100-µs pulses [2, 6], we choose 0.1 ms to estimate maximum temperature rise in our model.

Building a 3D geometry of tumor

In this study we used a 3D model of tumor and healthy tissue with needle electrode. Tumor geometry used in the numerical modeling for treatment planning purpose of IRE were constructed from MRI scans of a patient with Squamous cell carcinoma (SCC) that were provided in the Cancer Research Center, Tehran. The MR images were obtained using a 3 Tesla scanner (Trio, Siemens Medical Solutions, Erlangen, Germany), using 16 RF channels. Patient were administered Dotarem® via a hand injection (0.1 mmol/kg) over approximately 20 s. T2-weigthed imaging was started after 20 min of injection with following protocol: Turbo spin-echo with TE=117 ms, TR=750 ms, flip angel= 170˚ and voxel dimension of $0.5\times0.5\times0.5$ mm^3. The MRI data was imported into MIMICS (Materialize, Leuven, Belgium) software where tissues of interest were identified (Figure 1). Following automatic and manual manipulation of the structure, the geometry was transferred to Femlab software in order to numerical modeling.

Electrode geometry

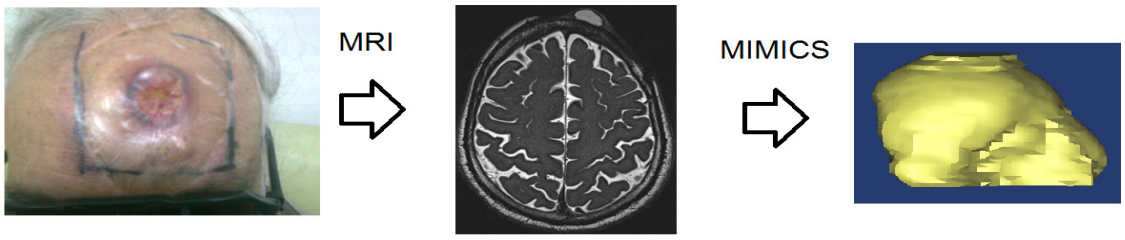

Figure 1: Volume rendering of patient's tumor using MRI data.

In this study we modeled 2-electrode geometry that used commonly in RE and IRE surgery. The electrodes were modeled as cylinders of sizes like to those used in various studies [7, 22]. We select 4 essential geometric and electric parameters for optimization as following: electrode thickness (t), distance between electrodes (d), insertion of electrodes in tissue (i), and electrode voltage (v). This parameter is shown in Figure 2 schematically.

Genetic algorithm

Genetic algorithm (GA) is a nature-based stochastic computational technique. The major advantages of GA is its broad applicability, flexibility and ability to obtain optimal solutions[23]. GA, initiated by J.Holland(1975), have confirmed useful in a variety of search and optimization problems in engineering, science and commerce[24]. The algorithm is based on the survival of the fittest which tries

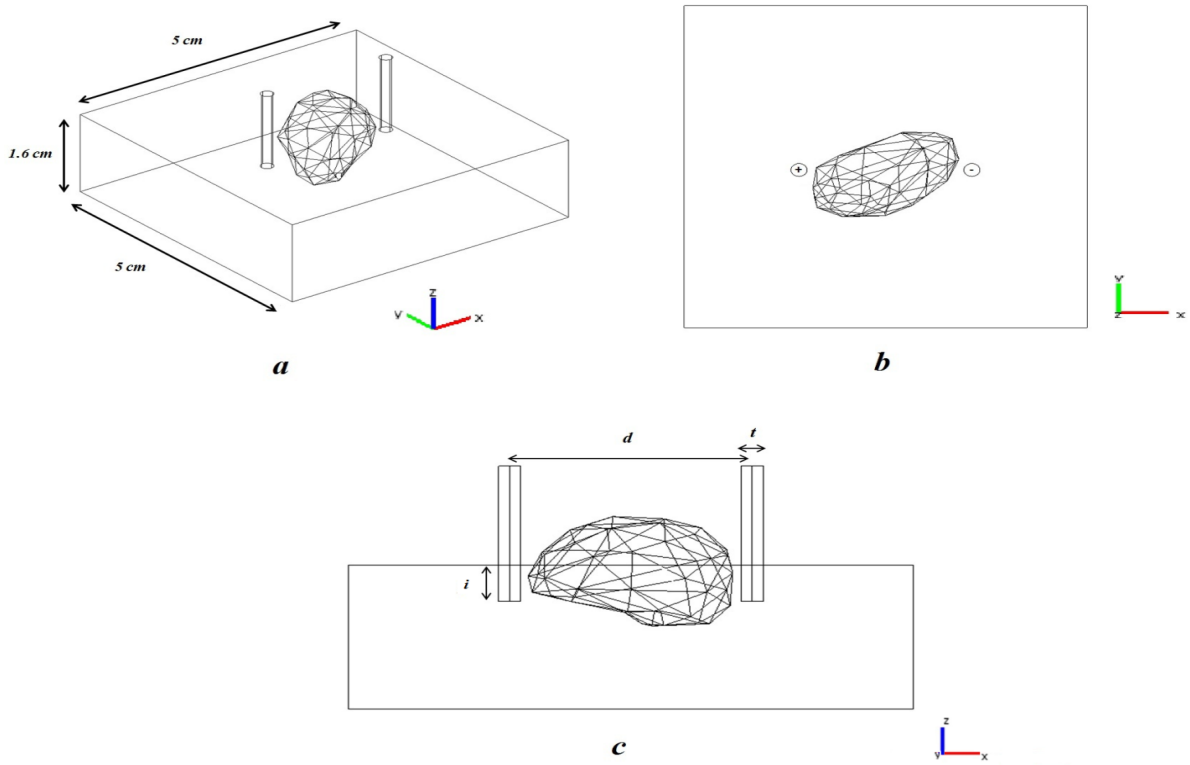

Figure 2: 3D geometry of tumor with cylindrical electrode. a) the surrounding healthy tissue around tumor b) x-y view of the model. the + and - sign represents the polarity of applied voltage(v). c) z-x view and geometric parameters of the model.

to maintain genetic information from generation to generation. To execute a GA optimization, a population of initial solutions must first be generated randomly. GA is an iterative algorithm where each iteration has two steps, the evaluation of fitness function step and the generation step. In the evaluation of fitness function step, the value of fitness function was evaluated. In generation step two individuals (parents) with maximum (or minimum) value for fitness function are chosen from the population. The selected parents are recombined to form two children, with two mechanisms of crossover and mutation [23, 25-27]. This procedure can be repeated until stopping criterion has been satisfied. This procedure is shown in Figure 3.

The genetic algorithm was written in Matlab R2010a (Mathworks, USA) and was coupled with the finite element models using the link between Matlab and Femlab software. In this study we used real coded multi-objective genetic algorithm (MOGA) in order to optimize electric and thermal distribution in tumoral

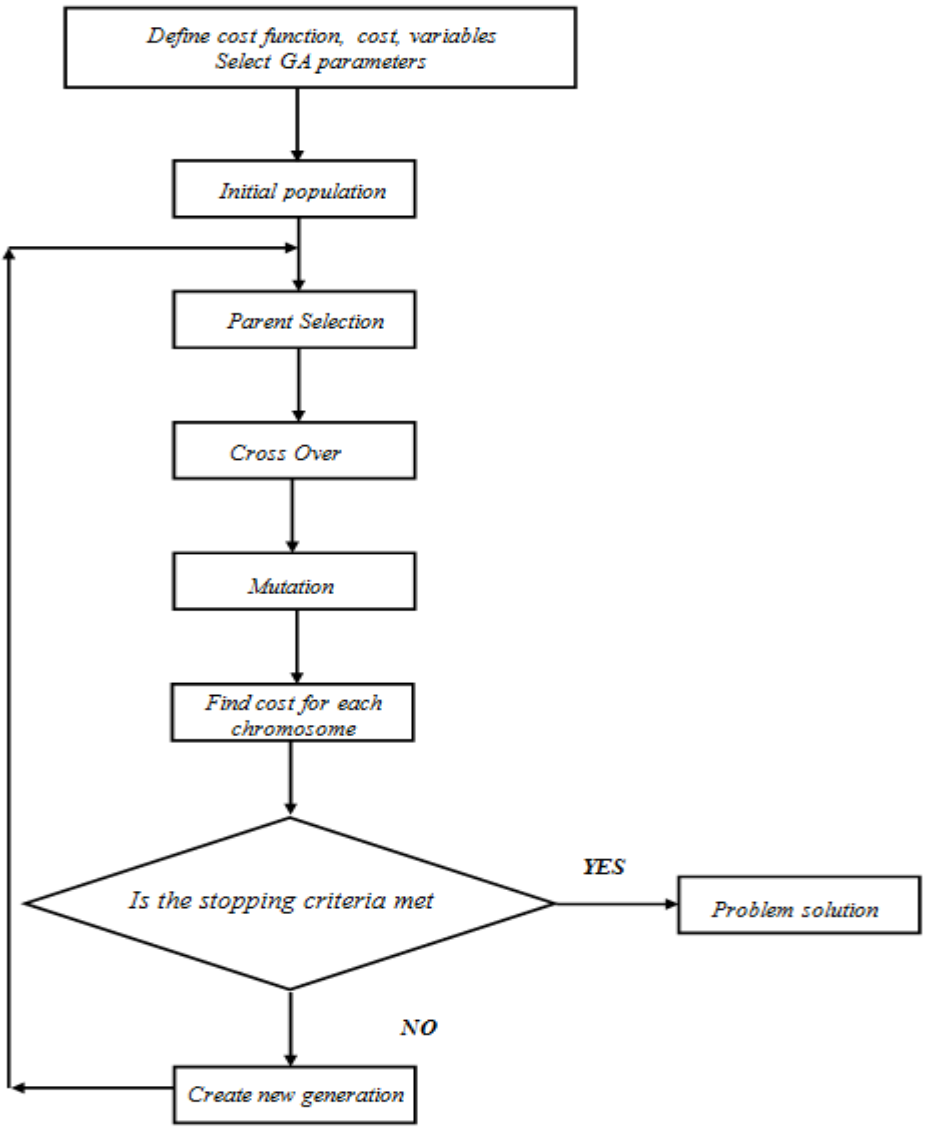

Figure 3: Flowchart of applied Genetic Algorithm

and healthy tissue. The written algorithm was validated using common test function (Table 2).

The mentioned functions in Table 2 have many local minimum with a global minimum and the written GA must find global minimum.

After validation, the main optimization was started. At first, initial population of solutions was generated randomly considering constraints for each parameter (t, d, i and v). These constraints (Table 3) were chosen in order to keep the solutions in real domain size. Such constraints come from tumor shape and clinical considerations. Initial population consists of specified number of individuals (chromosome). Each chromosome in population consists of 4 different variables (genes)(Figure 4). Each gene contains specified value for the variables in Table 3.

Table 2: Test function used in this study (all function were minimized).

Function name	No. of variables	Variable Bounds	Test function	Optimal Solution
Ackley(ACK)	n†	$-30 < x_i < 30$	$f(x_i) = -20e^{-0.2\sqrt{\frac{1}{n}\sum_{i=1}^{n} x_i^2}} - e^{\frac{1}{n}\sum_{i=1}^{n}\cos(2\pi x_i)} + 20 + \varepsilon, \quad , \quad i = 1,2,3,...n$	$x_i=0$, $f(x_i)=0$
Griewank(GWK)	n†	$-600 < x_i < 600$	$f(x_i) = \frac{1}{4000}(\sum_{i=1}^{n} x_i^2) - (\prod_{i=1}^{n} \frac{x_i}{\sqrt{i}}) + 1, \quad , \quad i = 1,2,3,...n$	$x_i=0$, $f(x_i)=0$
Hump(HUM)	2	$-5 < x_i < 5$	$f(x_1,x_2) = 4x_1^2 - 2.1x_1^4 + \frac{1}{3}x_1^6 + x_1x_2 - 4x_2^2 + 4x_2^4, \quad i = 1,2$	$x_1=\pm 0.0898$, $x_2=\pm 0.7126$ $f(x_i)=0$
Michalewicz(MCZ)	n†	$0 < x_i < \pi$	$f(x_i) = (\sum_{i=1}^{n} \sin(x_i)(\sin(\frac{ix_i^2}{\pi}))^{2m}, \quad i = 1,2,3,...n, m = 10$	$x_1=2.2$, $x_2=1.57$ $f(x_i)=-1.8013$
Rastrigins(RGN)	n†	$-5.12 < x_i < 5.12$	$f(x_i) = \sum_{i=1}^{n} x_i^2 - 10\cos(2\pi x_i) + 10, \quad i = 1,2,3,...n$	$x_i=0$, $f(x_i)=-10$
Shubert(SHT)	2	$-10 < x_i < 10$	$f(x_1,x_2) = \sum_{j=1}^{5} j\cos[(j+1)x_1 + j] \times \sum_{j=1}^{5} j\cos[(j+1)x_2 + j], \quad i = 1,2$	‡, $f(x_i)=-186.7309$

† These functions were solve for n=2.
‡ This function have 18 global minimum.

The fitness functions were defined as following: 1-normalized volume of tumor with E>900 V/cm (E-T), 2- normalized volume of healthy tissue with E>900 V/cm (E-H), 3-thermal damage of tumor (Ω-T) and 4- thermal damage of healthy tissue (Ω-H). The aim of optimization was E-T to be maximized and E-H, Ω-T and Ω-N to be minimized. E and Ω value for tumor or healthy tissue was calculated with solving eq. 1 and 2 respectively then using post processing features in Femlab software. The optimization was performed for each of mentioned fitness function (one-objective optimization). Moreover as prefect tumor coverage is crucial for treatment response, E-T

Table 3: Constraints of problem parameters (variables).

parameter	unit	Variable Bounds
t(electrode thickness)	mm	0.5-2
d(distance between electrodes)	mm	18-50
i(electrode insertion)	mm	0-1.6
v(voltage)	V	500-4000

was optimizes with other fitness function simultaneously (two-objective optimization). It should be noted in both one and two-objective optimization, final results are the best solutions among all generations.

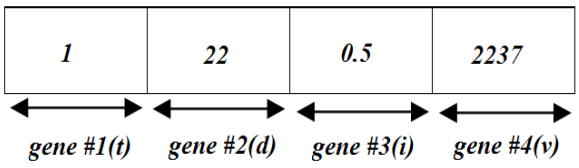

Figure 4: An individual (chromosome) in the population. Each chromosome consists of 4 genes. The defined fitness function evaluates for each chromosome.

The GA parameters can be found in Table 4. These parameters were optimized with both test function in Table 2 and problem fitness function. After the last generation, the fitness (or test) function reached a plateau and the algorithm was terminated.

Results

In Figure 5 the results for GA validation are shown. The results show the written GA is able to converge all of the test function in Table 2. In all cases the variance in five runs is also small.

Figure 6 gives the one-objective optimization results for each of the 4 fitness function. The optimization parameters were set corroding to Table 4. The results show the algorithm

Table 4: The GA parameters

Population size	No. of generation	Cross over rate	Mutation rate
60	150	0.8	0.1

was converged in all cases. Each point in the graph, associated with a value for electrode thickness (t), distance between electrodes (d), electrode insertion (i) and applied voltage (v). Table 5 presents the optimized parameters for each fitness function as well as fitness function values.

According to Table 5 just maximization of E-T can cover tumor with electric field greater than 900 V/cm perfectly leading to considerable damage to the healthy tissue. Although other minimization can minimize thermal damage to both healthy and tumoral tissue and electrical damage to healthy tissue, these optimization could not ablated tumor at all. In order to consider both tumor coverage and minimum damage simultaneously; two-objective optimization was performed.

The results of two-objective optimization are presented in Figure 7. Like Figure 6 each point in Pareto-front of the problem, associated with a value for 4 problem parameters (t, d, i and v). With increasing the tumor coverage with electric field greater than 900 V/cm (vertical axis), electrical damage to healthy tissue and thermal one to both healthy and tumoral tissue (horizontal) were increased (Figure 7). But as show in Figure 7; with two-objective optimization it is possible to choose parameters that can improve tumor coverage ratio regarding minimal electrical and thermal damage. The optimized parameters and associated fitness function values are tabulated (Table 6).

Discussion

The simulations showed that the magnitude of electric field intensity falls rapidly as we go away from the electrode surfaces. Furthermore the area with the maximum electric field strength (and temperature) was in the vicin-

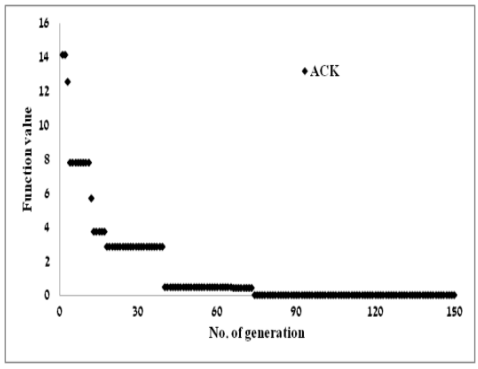

a

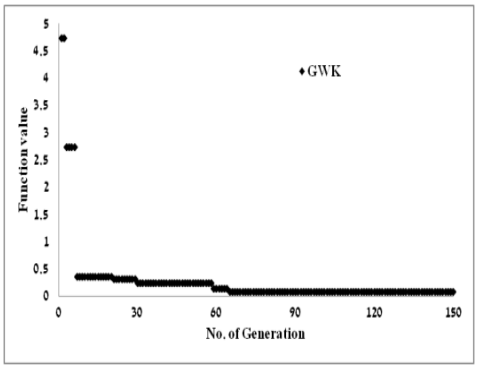

b

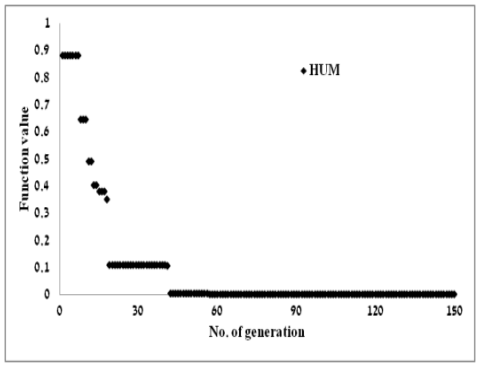

c

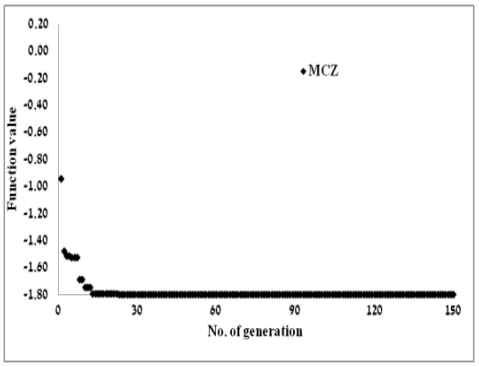

d

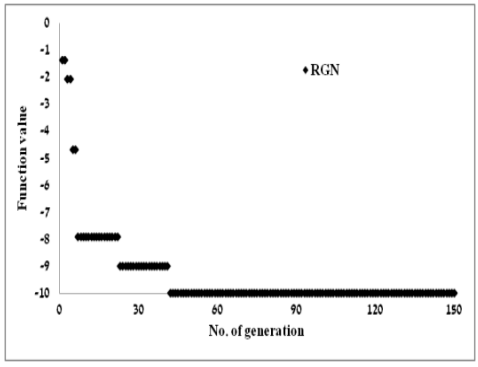

e

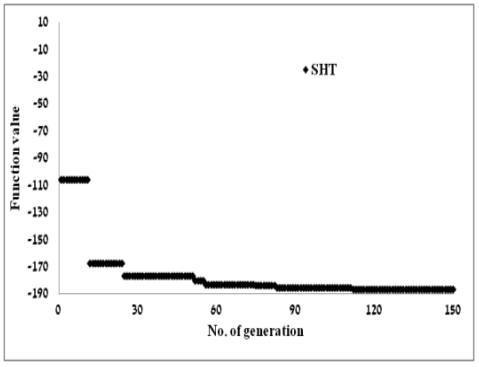

f

Figure 5: Convergence behavior of the GA for a) Ackley b) Griewank c) Hump d) Michalewicz e) Rastrigins f) Shubert functions. In all cases the algorithm converged before 120 th generation.

Table 5: Calculated values of problem parameters after one-objective optimization for E-H, E-T, Ω-H and Ω-T. After final result, the fitness function values were evaluated for the obtained parameters for each optimizatian.

					Final value of fitness function			
	t(mm)	d(mm)	i(mm)	v(V)	E-H	E-T	log(Ω-H)	log(Ω-T)
E-H†	0.7	44.2	7.6	504	0	0	-11.59	-11.72
E-T‡	1.5	22.0	9.9	3958	0.36	1	-9.91	-7.80
Ω-H†	0.5	44.4	0.5	541	0	0	-11.69	-11.7
Ω-T†	0.6	47.7	4	522	0.001	0	-11.47	-11.71

† The function was minimized.
‡ The function was maximized.

Table 6: Calculated values of problem parameters after two-objective optimization. The fitness function values were evaluated for the one of the best solutions that was shown in Figure 7 with arrow.

					Final value of fitness function			
	t(mm)	d(mm)	i(mm)	v(V)	E-H	E-T	log(Ω-H)	log(Ω-T)
E-T and E-H	0.61	21.03	7.52	3843	0.16	0.98	-11.17	-10.36
E-T and Ω-T	1.55	21.34	12.9	2812	0.36	0.99	-9.91	-10.90
E-T and Ω-H	0.56	21.17	7.23	3910	0.17	0.99	-11.25	-11.30

ity of electrodes and the area about them. In fact, the regions with the largest electric fields occur in the space between two electrodes. Therefore this region is crucial for considering both electric and thermal analysis.

Concerning GA optimization, it is not possible to consider both thermal and electrical aspect of IRE surgery with one-objective optimization. As mentioned in Table 5 the calculated parameters for maximization of E-T leads to significant electric damage to healthy tissue. Such parameters can produce dramatic temperature increases in the vicinity of electrodes. But due to rapid decrease of temperature away from electrode, there is no considerable thermal damage in healthy and tumoral tissue. Such problems also exist for other one-objective optimization. In fact minimization of E-H can lead to no part of tumor irreversibly electroporated. However it is possible to control such problems with two-objective optimization. Such optimization can preferentially ablate tumor tissue, preserving normal tissue at the treatment region considering two fitness functions (Pareto-front). Pareto-front is the solutions that cannot be improved in one-objective optimization. A complete representation of Pareto solutions is only possible using calculation of fitness value for each solution. It should be noted the solution are selected depending on which function is more important. For example if we want to ablate tumor with

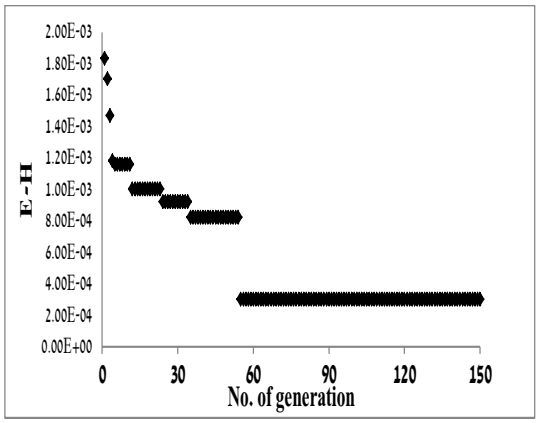

a

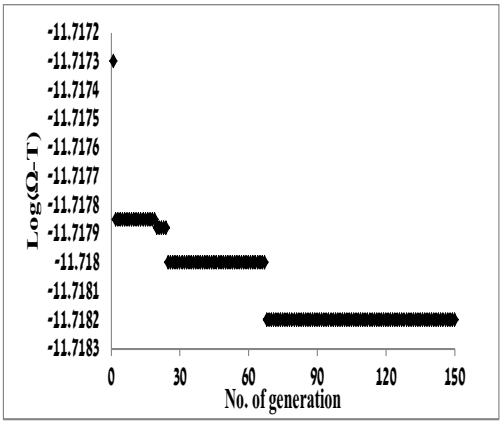

d

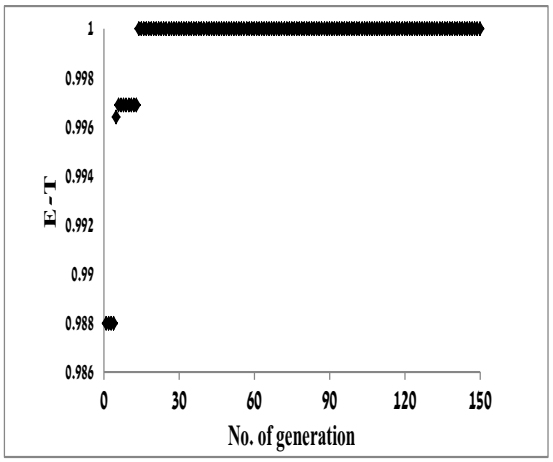

b

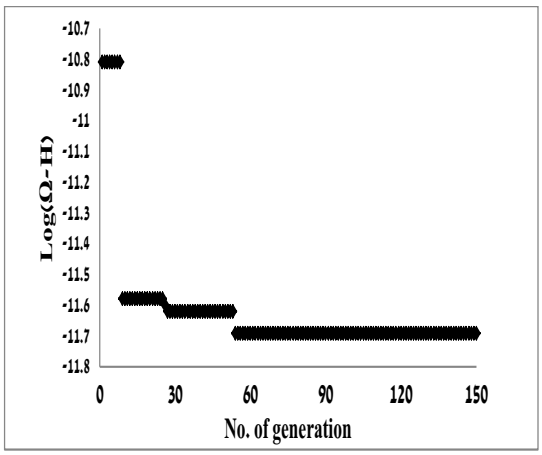

c

Figure 6: one-objective optimization for a) normalized volume of healthy tissue with E>900 V/cm, b) normalized volume of tumor with E>900 V/cm, c) logarithm of thermal damage to healthy tissue d) logarithm of thermal damage to tumor. a, c and d were minimized and b was maximized.

minimum electric damage to healthy tissue, we must use Figure 7a. All associated chromosome in plateau region near E-T=1 lead to prefect tumor ablation. Therefore if we choose a point with E-T=1 with less value for E-H, the consequent irreversibly electroporated area in healthy tissue becomes minimum. The similar argument exists for figures 7b and c.

We demonstrated that using multi-objective optimization result in prefect tumor ablation as well as minimum thermal/electrical damage. The nature of the genetic programming allows it to optimize functions with large number of parameters such as fitness functions in this study. Such approach can be used in IRE surgery as a treatment planning system to help physician choose the best treatment parameters.

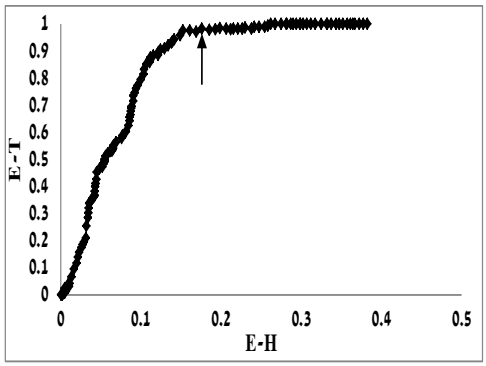

a

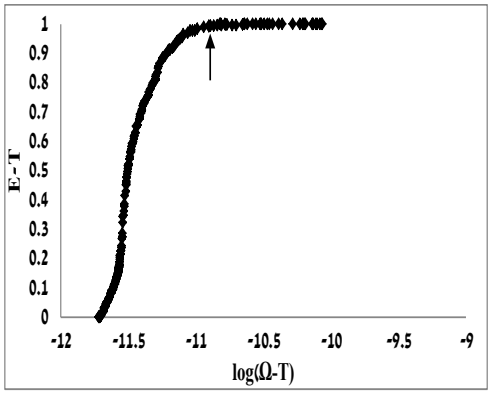

b

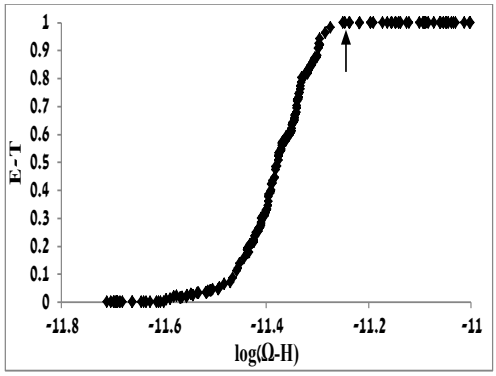

c

Figure 7: Pareto-front of two-objective optimization. The arrow represents region with a) maximum tumor converge with minimum electrical damage to healthy tissue b) maximum tumor converge with minimum thermal damage to tumor and c) maximum tumor converge with minimum thermal damage to healthy tissue.

References

1. Davalos RV, Mir IL, Rubinsky B. Tissue ablation with irreversible electroporation. *Ann Biomed Eng* 2005; 33(2): 223-31.
2. Maor E, Ivorra A, Rubinsky B. Non thermal irreversible electroporation: novel technology for vascular smooth muscle cells ablation. *PLoS One* 2009; 4(3): e4757.
3. Al-Sakere B, André F, Bernat C, Connault E, et al. Tumor ablation with irrevers-ible electroporation. *PLoS One* 2007; 2(11): e1135.
4. Rubinsky B, Onik G, Mikus P, Irreversible electroporation: a new ablation modality -clinical implications. *Technol Cancer Res Treat* 2007; 6(1): 37-48.
5. Lavee J , Onik G, Mikus P, Rubinsky B. A novel nonthermal energy source for surgical epicardial atrial ablation: irreversible electroporation. *Heart Surg Forum* 2007; 10(2): E162-7.
6. Maor E, Ivorra A, Leor J, Rubinsky B. The effect of irreversible electroporation on blood vessels. *Technol Cancer Res Treat* 2007; 6(4): 307-12.
7. Edd JF, Davalos RV. Mathematical modeling of irreversible electroporation for treatment planning. *Technol Cancer Res Treat* 2007; 6(4): 275-86.
8. Pavselj N, Miklavcic D. A numerical model of permeabilized skin with local transport regions. *IEEE Trans Biomed Eng* 2008; 55(7): 1927-30.
9. Pavselj N, Preat V, Miklavcic D. A numerical model of skin electropermeabilization based on in vivo experiments. *Ann Biomed Eng* 2007; 35(12): 2138-44.
10. Pavselj N , Miklavcic D. Numerical modeling in electroporation-based biomedical applications. *Radiology and Oncology* 2008; 42(3): 159-168.
11. Davalos RV ,Rubinsky B. Temperature considerations during irreversible electroporation. *International Journal of Heat and Mass Transfer* 2008; 51(23-24): 5617-5622.
12. Corovic S, Zupanic A, Miklavcic D. Numerical modeling and optimization of electric field distribution in subcutaneous tumor treated with electrochemotherapy using needle electrodes. *IEEE Transactions on Plasma Science* 2008; 36(4): 1665-1672.
13. Pavselj N, Bregar Z, Cukjati D, Batiuskaite D, Mir LM, Miklavcic D. The course of tissue permeabilization studied on a mathematical model of a subcutaneous tumor in small animals. *IEEE Trans Biomed Eng* 2005; 52(8): 1373-81.
14. Semrov D, Miklavcic D. Calculation of the electrical parameters in electrochemotherapy of solid tumours in mice. *Comput Biol Med* 1998; 28(4): 439-48.

15. Pennes, HH, Analysis of tissue and arterial blood flow temperatures in the resting forearm. *J App Physiol* 1948; 1: 93-122.
16. Shafirstein G, Novák P, Moros EG, et al. Conductive interstitial thermal therapy device for surgical margin ablation: In vivo verification of a theoretical model. *International Journal of Hyperthermia* 2007; 23(6): 477-492.
17. Duck FA. *Physical Properties of Tissues: A Comprehensive Reference Book.* Academic Press 1990.
18. Majchrzak E, Paruch M. *Numerical modelling of the cancer destruction during hyperthermia treatment, in Computer Methods in Mechanics* 2011: Warsaw, Poland.
19. Wilson SB, VA Spence. A tissue heat transfer model for relating dynamic skin temperature changes to physiological parameters. *Physics in Medicine and Biology* 1988; 33(8): 895.
20. He Y, Shirazaki M, Liu H, Himeno R, Sun Z. A numerical coupling model to analyze the blood flow, temperature, and oxygen transport in human breast tumor under laser irradiation. *Computers in Biology and Medicine* 2006; 36(12): 1336-1350.
21. Wainwright P. Thermal effects of radiation from cellular telephones. *Phys Med Biol* 2000; 45(8): 2363-2372.
22. Sel D, Cukjati D, Batiuskaite D, Slivnik T, Mir LM, Miklavcic D. Sequential finite element model of tissue electropermeabilization. *IEEE Trans Biomed Eng* 2005; 52(5): 816-27.
23. Gen M , R. Cheng R. *genetic algorithms and engineering optimization* 2000, New York: A JOHN WILEY & SONS, INC.
24. Goldberg DE. *Genetic algorithms in search, optimization, and machine learning* 1988, Reading, Mass.: Addison-Wesley Pub. Co.
25. Mitchell M. *An introduction to genetic algorithms* 2002, New Delhi: Prentice Hall of India.
26. Haupt RL, Haupt SE. *practical genetic algorithms.* 2nd ed1998, Hoboken, New Jersey.: A JOHN WILEY & SONS, INC.
27. Chambers, L., *practical hand book of genetic algorithm* Vol. 2. 1995, Perth: CRC Press.